Liquid Crystalline Poly(vinyl ether)s and Block Copoly(vinyl ether)s by Living Cationic Polymerization†

Michele Laus, Maria Chiara Bignozzi, Marco Fagnani, and Annino Sante Angeloni

Dipartimento di Chimica Industriale e dei Materiali, Viale Risorgimento 4, 40136 Bologna, Italy

Giancarlo Galli and Emo Chiellini*

Dipartimento di Chimica e Chimica Industriale, Via Risorgimento 35, 56126 Pisa, Italy

Oriano Francescangeli

Dipartimento di Scienze dei Materiali e della Terra, Via Brecce Bianche, 60131 Ancona, Italy

Received October 31, 1995; Revised Manuscript Received April 23, 1996⊗

ABSTRACT: A series of liquid crystalline (LC) poly(vinyl ether)s **1** was prepared by living cationic polymerization of a mesogenic vinyl ether monomer, 4-butoxyphenyl 4-((6-vinylhexyl)oxy)benzoate (**11**), in the presence of the HI/I_2 (1/1 mol/mol) initiating system. The number average molar mass of polymers **1** increased linearly with the initial monomer to initiator molar ratio (M_n = 3000−15 000 g mol^{-1}, $DP_n \approx 5-50$), according to the living character of the polymerization, and their molar mass distribution was rather narrow (M_w/M_n = 1.10−1.15). Furthermore, two sets of AB diblock copoly(vinyl ether)s **2** and **3** were prepared by sequential polymerization of vinyl ether **11** and isobutyl vinyl ether (**12**) and chiral (*S*)-2-methylbutyl vinyl ether (**13**) respectively, by using the same HI/I_2 system. While the average degree of polymerization of the LC block was kept constant ($DP_n \approx 10$), the length of the non-LC block was varied ($DP_n \approx 2-25$), according to the chosen feed conditions. An X-ray investigation proved that polymers **1** gave rise to a sequence of ordered smectic (F or I), smectic C, and nematic mesophases with increasing temperature. Their transition temperatures and entropies followed slightly different molar mass dependences, but each of them reached a saturation value at $M_n \approx 6000$ g mol^{-1}. The same basic mesophase polymorphism was also observed for the LC block copolymers **2** and **3**, thus suggesting that the chemically different blocks were microphase separated within the solid and LC phases.

Introduction

Considerable attention is being given to the molecular design of monomers and the synthesis of different liquid crystalline (LC) polymers to produce materials with optimized structures and defined architectures suitable for a variety of advanced applications.[1] In this respect, efforts of macromolecular engineering have been directed to developing polymeric materials with controlled molar mass characteristics and predetermined monomer sequences, thus providing a very effective way of tuning the LC characteristics of the polymers to desired levels.

To fulfill these goals, different synthetic approaches have been adopted, including living polymerization techniques such as the group transfer polymerization[2] and the anionic[3] and cationic polymerizations.[4,5] A few reports concern the group transfer polymerization of mesogenic monomers, and generally, the resulting products have low molar masses. On the other hand, the living anionic polymerization can be applied to the preparation of well-defined LC polymers but is typically restricted to a limited number of vinyl monomers which should not bear functional groups. In contrast, the living cationic polymerization, e.g. of vinyl ethers, requires less drastic synthetic conditions with respect to those to be used in anionic polymerizations. In addition, a larger number of monomers, even containing polar substituents, can be successfully polymerized. Accordingly, the living cationic polymerization represents a very effective and fairly straightforward tool of tailoring the structure and properties of LC polymers and can allow the preparation of block copolymers containing LC blocks. In spite of this fact, relatively little attention has been devoted to the preparation of LC poly(vinyl ether)s[4−9] and block copoly(vinyl ether)s.[10]

Diverse LC block copolymer architectures[2b,3b,10−15] have very recently been produced and are specially interesting for a number of reasons.[16] Due to the equilibrium nature of the LC phase transitions, the nature, onset, and stability of the mesophase of the LC block can in principle be correlated with the gross geometrical and topological characteristics of the block copolymer, such as the dimensions and shape of the domain structure, as well as the relevant interfacial contributions. In a complementary fashion, the distinct morphological environment, including the boundary conditions and finite size of the LC domains, can substantially affect the nature and stability of the microseparated LC phases.

From a practical point of view, the combination in one single polymer structure of the orientational and positional orders at the molecular level typical of liquid crystals and the compositional supermolecular order typical of block copolymers can lead to self-supported LC polymeric materials of considerable interest, in preparing for example multilayer nanostructures for microelectronics or ultrathin organic films for optical applications.

To widen further the molecular engineering of side chain LC polymers, this work reports on the synthesis by living cationic polymerization and LC behavior of a series of polymers **1**. These samples were obtained by

†Presented in part at the 35th IUPAC Symposium on Macromolecules, Akron OH, 1994.

⊗ Abstract published in *Advance ACS Abstracts,* June 1, 1996.

S0024-9297(95)01641-X CCC: $12.00

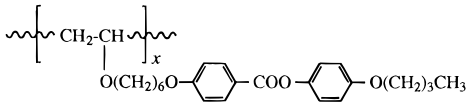

1

1	a	b	c	d	e	f
x	5	7	10	15	20	50

polymerizing an LC vinyl ether monomer using the HI/I_2 (1/1 mol/mol) initiating system, and their molar mass was controlled ($x \approx 5-50$) by varying systematically the initial monomer/initiator molar ratio ($[M]_0/[I]_0$). In addition, to test the suitability of the living cationic polymerization in the synthesis of LC block copolymers, we prepared and studied two block copolymer systems **2** and **3**.

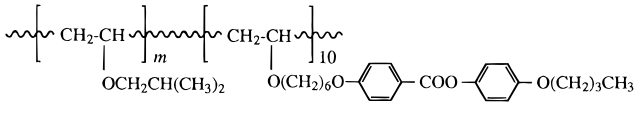

2

2	a	b	c	d
m	2	3	10	25

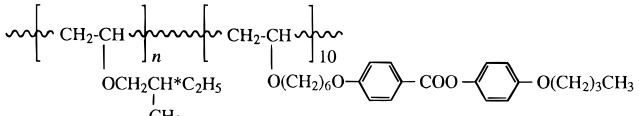

3

3	a	b
n	10	25

AB diblock copolymers **2** and **3** are constituted by the same vinyl ether block as in homopolymers **1** ($DP_n \approx 10$) and a block derived from isobutyl vinyl ether and (*S*)-2-methylbutyl vinyl ether with different lengths m ($m = 2-25$) and n ($n = 10, 25$), respectively.

Experimental Section

Materials. Toluene and hexane were washed with 2 M potassium carbonate, 2 M sulfuric acid, and water and then distilled under dry argon, twice over calcium hydride and once over sodium immediately before use. Hydrogen iodide was obtained from a 57% aqueous solution (Aldrich) by dehydration with phosphorus pentoxide and stored as a hexane solution in a sealed ampule at −40 °C. Iodine (Aldrich, guaranteed reagent, purity >99.9%) was used without further purification as a toluene solution. The molarities of the hydrogen iodide and iodine solutions were determined by acid−base back-titration and sodium thiosulfate titration, respectively.

6-Chloro-1-hexanol (**4**) and butyl vinyl ether (**5**) were used as received. Isobutyl vinyl ether (**12**) was washed with 2 M potassium carbonate, 2 M sulfuric acid, and water, dried on anhydrous sodium sulfate, and then distilled under dry argon, twice over calcium hydride and once over sodium/potassium alloy immediately before use. (*S*)-2-Methylbutyl vinyl ether (**13**) was prepared according to the literature[17] and distilled over sodium immediately before use (bp 111−112 °C; $[\alpha]^{25}_D = +6.7°$ (neat)).

4-((Benzyloxycarbonyl)oxy)benzoic acid (**7**) was synthesized according to the literature.[18]

1-Chloro-6-(vinyloxy)hexane (6). A mixture of 29.9 g (219 mmol) of **4**, 157.0 g (1580 mmol) of **5**, and 11.7 g (37.0 mmol) of mercuric acetate was refluxed under stirring for 6 h, and then 15 g of dry potassium carbonate was added. The solution was filtered, and the unreacted **5** was distilled off. The residue was purified by fractional distillation to give **6**. Yield: 45%. Bp: 65−68 °C/4 mbar.

^{1}H NMR ($CDCl_3$): δ = 6.4 (dd, 1H, HC═), 4.1 and 3.9 (2 dd, 2H, H_2C═), 3.6 (t, 2H, OCH_2), 3.5 (t, 2H, CH_2Cl), 1.8−1.3 (m, 8H, $(CH_2)_4$).

4-Butoxyphenyl 4-((Benzyloxycarbonyl)oxy)benzoate (9). A mixture of 21.9 g (80.5 mmol) of **7**, 15 mL (206 mmol) of thionyl chloride, 2−3 drops of pyridine, and 40 mL of anhydrous dichloroethane was refluxed under dry argon, until a transparent solution was obtained. The solvent and excess of thionyl chloride were vacuum distilled in the presence of anhydrous benzene to give the solid acid chloride. This was dissolved under dry argon in 20 mL of anhydrous dichloroethane and rapidly added to a solution of 13.3 g (80.5 mmol) of 4-butoxyphenol (**8**) and 1.0 g (2.80 mmol) of benzyltributylammonium bromide in 100 mL of 1 M sodium hydroxide. The reaction mixture was vigorously stirred for 15 min. The organic phase was separated and washed with 0.5 M sodium hydroxide and water, dried over anhydrous sodium sulfate and evaporated to dryness. The solid residue **9** was crystallized from absolute ethanol. Yield: 70%. Mp: 95−96 °C.

^{1}H NMR ($CDCl_3$): δ = 8.2 (dd, 2H, arom), 7.5−7.2 (m, 11H, arom), 5.3 (s, 2H, $ArCH_2O$−), 3.9 (t, 2H, $ArOCH_2$−), 1.8−1.3 (m, 4H, $-CH_2-$), 1.0 (t, 3H, $-CH_3$).

4-Butoxyphenyl 4-Hydroxybenzoate (10). A suspension of 23.7 g (56.3 mmol) of **9** and 0.5 g of 10% Pd−C in dry tetrahydrofuran was treated with hydrogen in a Parr apparatus at 2.5 kg cm^{-2} pressure at room temperature until no more hydrogen was consumed. The reaction mixture was filtered and the solvent evaporated under vacuum. The solid product **10** was crystallized from benzene. Yield: 80%. Mp: 159 °C.

^{1}H NMR ($CDCl_3$): δ = 8.0 (dd, 2H, arom), 7.1 (dd, 2H, arom), 6.9 (dd, 4H, arom), 6.4 (s, H, −OH), 3.9 (t, 2H, $ArOCH_2$−), 1.8−1.3 (m, 4H, $-CH_2-$), 0.95 (t, 3H, $-CH_3$).

4-Butoxyphenyl 4-((6-Vinylhexyl)oxy)benzoate (11). A mixture of 12.9 g (45.1 mmol) of **10**, 7.3 g (45.1 mmol) of **6**, and 12.5 g (90.2 mmol) of dry potassium carbonate in 70 mL of dry dimethyl sulfoxide was heated to 90 °C under stirring. After 2 h, the mixture was poured into 200 mL of cold water under vigorous stirring and filtered. The residue was washed with 1 M NaOH and then water. The solid product was crystallized from 95% ethanol to give pure **11**. Yield: 70%. Mp: 71−73 °C.

^{1}H NMR ($CDCl_3$): δ = 8.1 (dd, 2H, arom), 7.1 (dd, 2H, arom), 6.9 (dd, 4H, arom), 6.4 (dd, 1H, CH═), 4.2 and 4.1 (2 dd, 2H, CH_2═), 4.0 (m, 4H, $-CH_2OAr$), 3.7 (t, 2H, $-OCH_2$), 1.8−1.4 (m, 12H, $-CH_2-$), 1.0 (t, 3H, $-CH_3$).

Poly(vinyl ether)s 1. All the polymerizations were carried out under dry argon using an experimental procedure similar to that described here for sample **1c** (Scheme 1). The reaction was initiated by adding in the order 1.0 mL of a 0.240 M hexane solution of hydrogen iodide prechilled at 0 °C and 6.5 mL of a 0.037 M solution of iodine in toluene prechilled at 0 °C to 42.5 mL of a 0.056 M toluene solution of monomer **11**, at the polymerization temperature of −40 °C. After 25 min, the polymerization was terminated by adding ammoniacal methanol prechilled at 0 °C. The quenched reaction mixture

Scheme 1

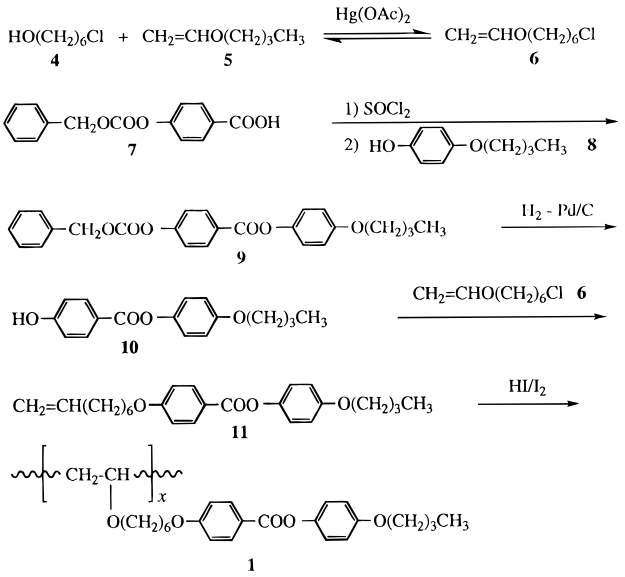

Table 1. Experimental Conditions and Average Molar Mass Data of Poly(vinyl ether)s 1

sample	$[M]_0/[I]_0$[a]	time/min	yield/%	M_n[b]/g mol^{-1}	M_w/M_n[b]
1a	5	25	80	3000	1.10
1b	7	35	78	3500	1.10
1c	10	60	83	4500	1.10
1d	15	80	80	6000	1.10
1e	20	300	81	7000	1.15
1f	50	1320	85	15000	1.15

[a] Initial monomer/initiator molar ratio; $[M]_0 = 0.048$ M. [b] By SEC, in chloroform at 25 °C.

Table 2. Experimental Conditions and Average Molar Mass and Composition Data of Block Copolymers 2 and 3

sample	R[a]	time/min	yield/%	**11** content[b]/ wt %	M_n[c]/g mol^{-1}	M_w/M_n[c]
2a	5/1	60	80	97 (95)	9000	1.30
2b	3/1	60	75	92 (93)	12000	1.35
2c	1/1	60	70	90 (80)	14000	1.40
2d	1/2.5	120	56	75 (62)	15000	1.40
3a[d]	1/1	60	85	79 (78)	6500	1.35
3b[e]	1/2.5	120	85	68 (59)	8000	1.40

[a] Molar ratio between vinyl ethers **11** and **12** (copolymers **2**) or **13** (copolymers **3**). [b] Copolymer content of counits from **11** by ^{1}H NMR (theoretical values in parentheses). [c] By SEC, in chloroform at 25 °C. [d] Optically active sample ($[\alpha]^{25}_D = 0.8°$ (chloroform)). [e] Optically active sample ($[\alpha]^{25}_D = 1.3°$ (chloroform)).

was washed with aqueous sodium thiosulfate and then water and evaporated to dryness under reduced pressure to give the polymer product. For a further purification, the polymer was precipitated several times from chloroform solution into methanol.

Six samples were synthesized using different monomer/initiator molar ratios $[M]_0/[I]_0 = 5$, 7, 10, 15, 20, and 50). Their concentration data, conversions, reaction times, and molar mass characteristics are collected in Table 1.

Block Copoly(vinyl ether)s 2 and 3. All the copolymerizations were carried out under the same conditions described for the synthesis of **1c**, employing in each experiment a ratio $[M]_0/[I]_0 = 10$. After about 30 min, **11** was consumed quantitatively and a second feed of isobutyl vinyl ether (**12**) (copolymers **2**) or (*S*)-2-methylbutyl vinyl ether (**13**) (copolymers **3**) was added to the reaction mixture. The second stage of the polymerization was completed in ca. 1 h. Four block copolymer samples **2** and two block copolymer samples **3** were prepared by varying the molar ratio R between the vinyl ethers **11** and **12** and between vinyl ethers **11** and **13**, respectively, as follows: $R = 5/1$, **2a**; $R = 3/1$, **2b**; $R = 1/1$, **2c**; $R = 1/2.5$, **2d**, and $R = 1/1$, **3a**, and $R = 1/2.5$, **3b**. The copolymerizations were terminated by adding prechilled ammoniacal methanol, and the copolymerization mixture was treated under the same conditions as for homopolymers **1**. In addition the copolymerization products were extracted with boiling ethanol to remove possible traces of poly(isobutyl vinyl ether) or poly((*S*)-2-methylbutyl vinyl ether). Experimental details, including yields and reaction times are collected in Table 2.

Characterization. ^{1}H NMR and ^{13}C NMR spectra were recorded on a Varian Gemini 200 spectrometer. The composition of the copolymers was determined from the relative areas of the different counit signals in the ^{1}H NMR spectra. Number average molar masses were determined by SEC of chloroform solutions with a 590 Waters chromatograph equipped with a Perkin-Elmer UV detector using a 10^3 Å Polymer Laboratories column and a Waters U6K injector. Polystyrene standard samples were used for the calibration.

Differential scanning calorimetry (DSC) analyses were carried out under dry nitrogen flow with a Perkin-Elmer DSC 7 apparatus. The temperature scale was calibrated against the melting temperature of indium. For the determination of the transition enthalpy, indium was used as a standard material. The transition temperatures were taken from the DSC traces of samples annealed by cooling from the isotropic melt, as corresponding to the maximum and to the onset point of the enthalpic peaks for polymers and low molar mass samples, respectively, at a heating rate of 10 K min^{-1}.

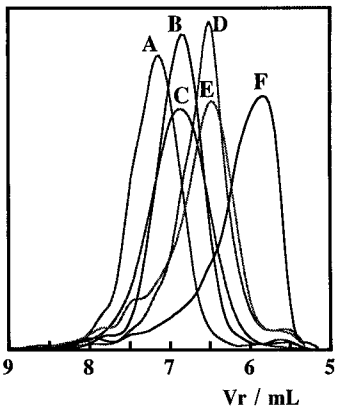

Figure 1. SEC curves of poly(vinyl ether)s **1a** (A), **1b** (B), **1c** (C), **1d** (D), **1e** (E), and **1f** (F).

X-ray diffraction measurements on powder samples were performed using the INEL CPS 120 powder diffractometer, equipped with a position sensitive detector covering 120° in the scattering angle 2θ, with an angular resolution of 0.018° in θ. Ge(111) monochromatized Cu Kα radiation, collimated with an appropriate system of slits, was used. X-ray diffraction photographs on oriented samples were obtained by means of a Rigaku-Denki RU300 rotating anode generator equipped with a pinhole flat camera. The primary beam of Ni-filtered Cu Kα radiation ($\lambda = 1.54$ Å) impinged on a ca. 1 mm thick sample, the temperature of which was controlled to ±0.1°. Fibers were oriented by pulling up with tweezers the viscous liquid crystalline melt.

Results and Discussion

Synthesis. Vinyl ether monomer **11** was synthesized according to the procedure outlined in Scheme 1. 1-Chloro-6-(vinyloxy)hexane (**6**) was prepared by reacting 6-chloro-1-hexanol (**4**) with excess butyl vinyl ether (**5**) in the presence of mercuric acetate. Phenol **10** was prepared by reacting 4-butoxyphenol (**8**) with the acyl chloride of 4-((benzyloxycarbonyl)oxy)benzoic acid (**7**) and removing the benzyloxycarbonyl group by catalytic hydrogenation. The final coupling reaction between **6** and **10** was performed in the presence of potassium carbonate in dry dimethyl sulfoxide.

LC poly(vinyl ether)s **1** and block copoly(vinyl ether)s **2** and **3** were synthesized by living cationic polymerization using the HI/I_2 (1/1 mol/mol) initiator.[19] Six samples of poly(vinyl ether)s **1** were prepared by polymerizing vinyl ether monomer **11** at −40 °C in toluene solution (Scheme 1). The polymerization yields were almost quantitative and reduced to about 80% after extensive purifications to eliminate residual initiator and unreacted monomer. The initial monomer concentration ($[M]_0$) was kept constant ($[M]_0 = 0.048$ M), whereas the monomer/initiator molar ratio ($[M]_0/[I]_0$) was systematically changed from 5 for **1a** to 50 for **1f**. The structure of poly(vinyl ether)s **1** was established by ^{1}H NMR and ^{13}C NMR. The molar mass characteristics were determined by size exclusion chromatography (SEC). Polymers **1** show monomodal SEC curves (Figure 1) that shift toward lower values along the elution volume scale as the molar ratio $[M]_0/[I]_0$ increases. Minor shoulders were also seen in the SEC curves of some polymer sample due to traces of polymer fractions with different molar masses. Number average molar masses (M_n) from 3000 to 15 000 g mol^{-1} and first polydispersity indexes (M_w/M_n) in the 1.10−1.15 range were evaluated, using directly the polystyrene calibra-

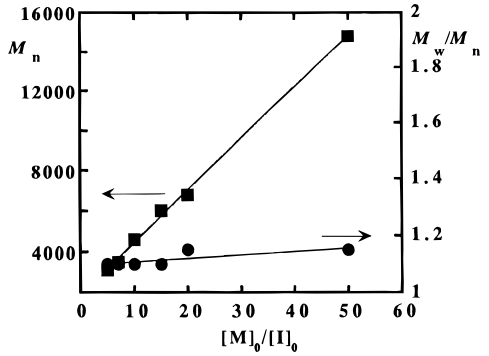

Figure 2. Trend of the number average molar mass (■) and first polydispersity index (●) of polymers **1** as a function of the monomer **11**/initiator molar ratio ($[M]_0/[I]_0$).

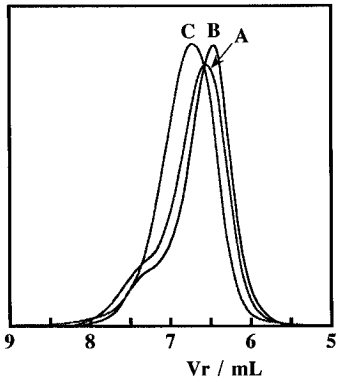

Figure 3. SEC curves of block copolymers **3a** (A) and **3b** (B) and homopolymer **1c** (C).

tion curve (Table 1). M_n increases linearly with $[M]_0/[I]_0$, as expected for a living cationic polymerization,[20] and the first polydispersity index is practically constant (Figure 2).

AB diblock copolymers **2** and **3** were prepared by sequential polymerization of vinyl ether monomer **11**, isobutyl vinyl ether (**12**), and (*S*)-2-methylbutyl vinyl ether (**13**), respectively, using HI/I_2 in toluene at −40 °C. In all cases a monomer **11**/initiator molar ratio ($[M]_0/[I]_0$) of 10 was employed, due to the finding that for this value the LC properties of the corresponding polymer **1** become essentially independent of M_n (see below). After about 30 min, **11** was consumed quantitatively, and on addition of a second feed of isobutyl vinyl ether (**12**) (copolymers **2**) or (*S*)-2-methylbutyl vinyl ether (**13**) (copolymers **3**), a second-stage polymerization ensued and was complete in approximately 1 h. This allowed the preparation of AB diblock copolymers. All the copolymers were precipitated several times from chloroform solution into methanol to eliminate unreacted monomers and were purified by selective extraction with boiling ethanol in which poly(isobutyl vinyl ether) and poly((*S*)-2-methylbutyl vinyl ether) are soluble. Only minor traces of these homopolymers were found, thus indicating a negligible incidence of chain transfer reactions during the copolymerization. The conversion of the vinyl ether monomers **12** and **13** ranged from 85 to 90%. Four block copolymer **2** samples and two block copolymer **3** samples were prepared by varying the molar ratio *R* between vinyl ethers **11** and **12** ($R = 5$, 3, 1, and 0.4) and between vinyl ethers **11** and **13** ($R = 1$ and 0.4), respectively (Table 2). Figure 3 illustrates the SEC curves of block copolymers **3a** and **3b** together with the one of **1c**, as representative examples. The SEC curves of the block copolymers are shifted toward lower values along the

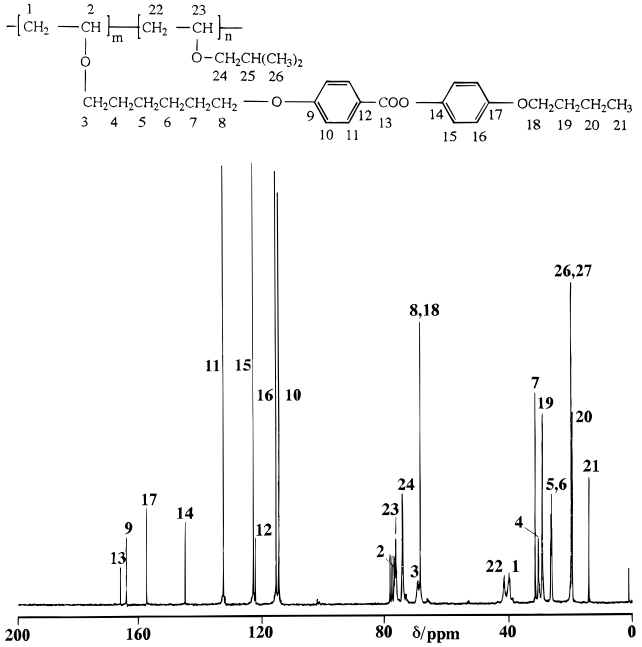

Figure 4. ^{13}C NMR spectrum of block copolymer **2d** in $CDCl_3$ solution.

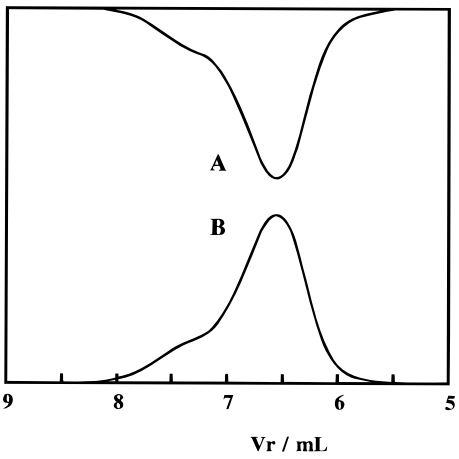

Figure 5. SEC curves of block copolymer **3a** as detected by refractive index (A) and ultraviolet (B) recordings.

elution volume scale with the increasing total monomer amount in the feed mixture. M_n varied from 9000 to 15 000 g mol^{-1} ($M_w/M_n = 1.30-1.40$) for samples **2** and from 6500 to 8000 g mol^{-1} ($M_w/M_n = 1.35-1.40$) for samples **3** (Table 2). The structure of the copolymers was established by ^1H NMR and ^{13}C NMR spectroscopy (Figure 4). Assignments of the various signals were made by combined chemical shift calculations and comparison of the spectra with those of the monomers and low molar mass intermediates. The block copolymer composition, as evaluated by ^1H NMR, is in good agreement with the one expected considering the living mechanism of the reaction (Table 2). An additional proof of block copolymer formation was obtained by SEC with dual detection by refractive index and ultraviolet recordings (Figure 5). The wavelength of 360 nm was used for the ultraviolet detector at which isobutyl vinyl ether and (*S*)-2-methylbutyl vinyl ether homopolymers are transparent. The SEC traces are practically superposable, thus showing the formation of a copolymer in which both blocks of different lengths are homogeneously distributed over the whole molar mass dispersion curve.

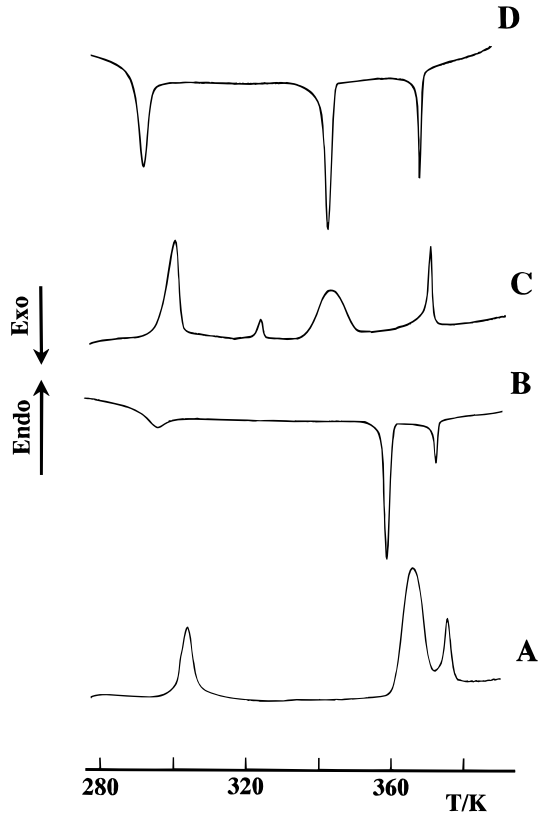

Figure 6. DSC second heating and first cooling curves (10 K min^{-1}) of polymers **1a** (C, D) and **1c** (A, B).

LC Properties. The phase transition temperatures and relevant thermodynamic parameters of monomer **11**, polymers **1**, and block copolymers **2** and **3** were determined by DSC. The nature of the LC phases was investigated by qualitative observations of the optical textures on the hot stage of a polarizing microscope and by X-ray diffraction. Monomer **11** melts at 344 K and shows a smectic C−isotropic transition at 360 K. An additional monotropic transition occurs at 343 K due to the formation of an unidentified smectic mesophase. The relevant entropies are 5.0 J mol^{-1} K^{-1} for the former LC transition and 5.4 J mol^{-1} K^{-1} for the latter.

Figure 6 shows the DSC heating and cooling curves of polymers **1a** and **1c** as typical examples. On heating **1a** (Figure 6C), three well-defined endothermic transitions are seen at 302, 345, and 368 K, that are reversible on cooling with a supercooling of a few degrees (Figure 6D). These transitions are attributed to three LC transitions. In addition, a low-intensity fourth endothermic peak is observed at 332 K in the heating curve preceded by a shallow exotherm. This last transition has no counterpart in the cooling curve and is attributed to the melting of crystalline regions grown during the heating scan. The thermal behavior of **1b** is similar to the one of **1a**. The other polymer **1** samples display DSC curves similar to those of **1c** (Figure 6A,B), in which there are only three endotherms (on heating) and three exotherms (on cooling) associated with the LC phase transitions. In these samples, the melting process is not apparent. This different behavior is possibly due to the differences in molar mass of the samples.

Figure 7 shows the X-ray powder diffraction patterns of **1f** recorded from room temperature up to the isotropization point. At room temperature (Figure 7A) the spectrum is constituted by a broad Bragg reflection in the small-angle region at a periodicity of ca. 22 Å and

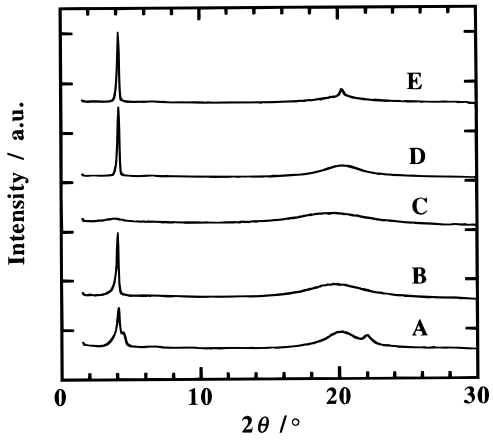

Figure 7. X-ray powder diffraction spectra of polymer **1f** recorded at different temperatures: 300 K (A, virgin sample); 320 K (B); 380 K (C); 300 K (D, after cooling from the isotropic melt); 300 K (E, after annealing for 20 h).

two diffuse signals in the wide-angle region corresponding to about 4 and 5 Å. The layer spacing $d \approx 22$ Å is much shorter than the length of the repeating unit in the fully extended conformation, $L = 31 \pm 0.5$ Å (as estimated from the Dreiding stereomodels), thus suggesting a monolayer tilted arrangement of the side-chain groups within smectic layers such as in a smectic C (S_C) mesophase. A tilt angle $\beta = 45 \pm 1°$ to the layer normal is evaluated. On heating, the small-angle Bragg diffraction sharpens ($d = 21.9$ Å) and the wide-angle signal becomes very diffuse at temperatures above 320 K (Figure 7B), corresponding to the temperature relevant to the first DSC endothermic transition. The broadening of the wide-angle peak indicates a loss of the lateral correlation among the molecular segments within the smectic layers. The resulting X-ray pattern does not change substantially up to 380 K (Figure 7C). Above this temperature, corresponding to the second DSC endothermic transition, the small-angle peak disappears, indicating the transition to the nematic (N) melt. On further heating, the isotropic (I) melt is eventually reached. The smectic interlayer spacing is practically constant from room temperature up to the S_C−N transition. Additional information was obtained from X-ray diffraction measurements on an oriented specimen as attained by drawing a fiber out of the mesophase at 350 K and quenching it. In the small-angle region (Figure 8), there are four Bragg spots corresponding to the first- and second-order reflections on the smectic layers. They are aligned on the equator, thus indicating that the smectic layers are parallel to the fiber axis. In addition, four diffuse spots in the wide-angle pattern are symmetrically placed around the direct beam, which indicates a liquid-like order within the layers. These diffuse spots are roughly equidistant from the origin and form pairs on straight lines making an angle $\beta \approx 42°$ with respect to the fiber axis. Therefore, we conclude that the mesogenic groups are tilted with respect to the layer normal by an angle $\beta \approx 42°$, in agreement with the results on powder samples. This clearly brings out the smectic C nature of the mesophase of polymers **1**. Annealing the fiber for 20 h at 300 K, that is just below the lowest temperature DSC endothermic transition, results in a significant sharpening of the wide-angle diffuse signal (Figure 7E), whereas no modifications of the small-angle Bragg peak are detected. This suggests the existence of a hexagonal packing of the mesogens within the smectic layers of either a smectic F (S_F) or a smectic I (S_I) mesophase, in

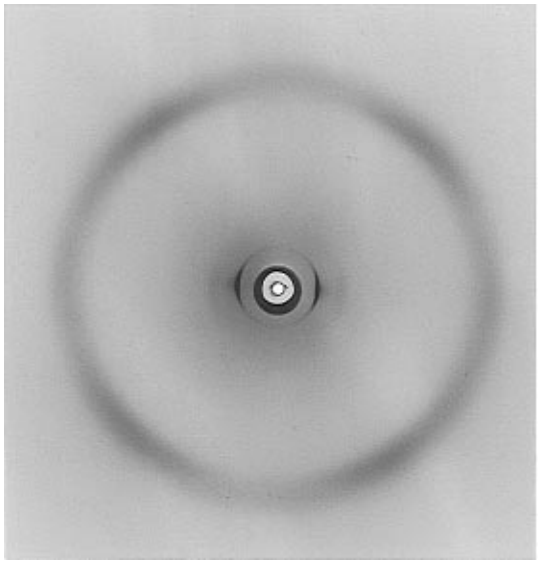

Figure 8. X-ray fiber diffraction pattern for the oriented smectic C mesophase of polymer **1c** (vertical fiber axis).

Table 3. Phase Transition Parameters[a] of Polymers 1

sample	$T_{S_X-S_C}$/ K	T_{S_C-N}/ K	T_{N-I}/ K	$\Delta S_{S_X-S_C}$/J mol^{-1} K^{-1}	ΔS_{S_C-N}/J mol^{-1} K^{-1}	ΔS_{N-I}/J mol^{-1} K^{-1}
1a	302	345	368	3.5	6.2	2.3
1b	302	354	370	3.4	7.5	2.2
1c	304	365	375	3.4	8.2	2.1
1d	304	366	376	3.5	8.2	2.2
1e	305	365	376	3.4	8.1	2.2
1f	320	379	384	4.3	7.6	1.9

[a] Transition temperatures and entropies (T, ΔS). Phases: S_X, smectic F or I; S_C, smectic C; N, nematic; I, isotropic.

which the tilt angle is the same as in the higher temperature S_C mesophase. It is difficult to distinguish the S_F phase (tilt direction toward an edge of the hexagon) from the S_I phase (tilt direction toward an apex of the hexagon), the latter mesophase being, however, characterized by a greater order of the mesogens within the smectic layers.[21,22] Accordingly, the mesophase sequence of polymers **1** can be summarized as follows:

$$S_{X(F\text{ or }I)} \rightarrow S_C \rightarrow N \rightarrow I$$

The transition temperatures (T) and entropies (ΔS) detected for samples **1** are collected in Table 3. The trends of the transition temperatures as a function of M_n are illustrated in Figure 9. The S_C-N temperature increases substantially with increasing M_n, whereas the S_X-S_C temperature and the N−I or isotropization temperature are quite insensitive to the molar mass. Above a saturation value at $M_n \approx 6000$ g mol^{-1}, all the transition temperatures remain constant. The trends of ΔS as a function of M_n closely parallel the ones of the transition temperatures (Figure 10). The influence of M_n on the transitional parameters of polymers **1** is in general agreement with that found for other polymeric systems,[23,24] although the degree of polymerization above which the phase transition parameters become independent of the molar mass is somewhat lower than the one reported for the majority of those polymeric systems.

The thermal data of the block copolymers are collected in Tables 4 and 5. The DSC heating and cooling curves of block copolymers **2d** and **3b** as representative examples of the two systems are reported in Figure 11. In the heating curve of **2d**, there are four endotherms at 302, 316, 352, and 361 K. The endothermic transition at 316 K is attributed to the melting of a poorly semicrystalline poly(isobutyl vinyl ether) block because of a low degree of stereoregularity. The other transitions are associated with the S_X-S_C, S_C-N, and N−I transitions of the LC poly(vinyl ether) block (Figure

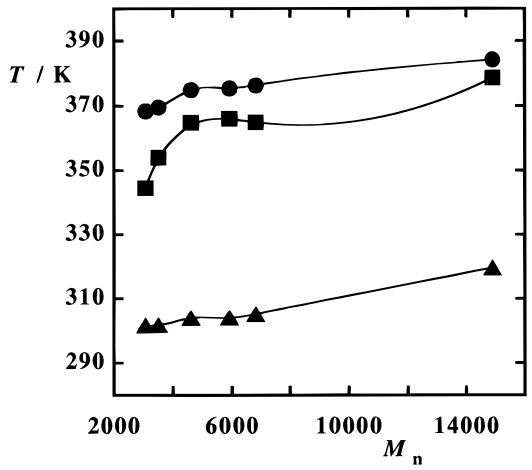

Figure 9. Trends of the smectic X−smectic C (▲), smectic C−nematic (■), and nematic−isotropic (●) transition temperatures as a function of M_n.

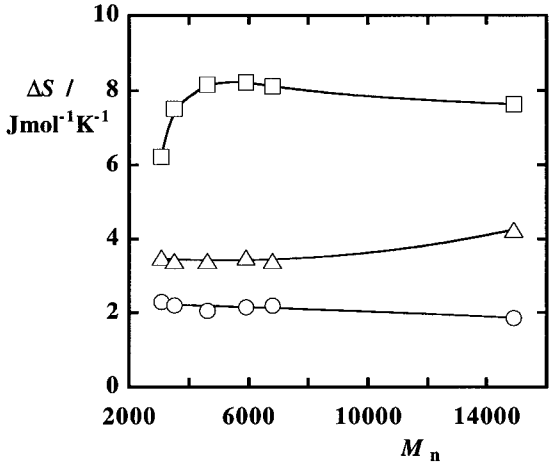

Figure 10. Trends of the smectic X−smectic C (△), smectic C−nematic (□), and nematic−isotropic (○) transition entropies as a function of M_n.

Table 4. Phase Transition Parameters[a] of Copolymers 2

sample	T_m[b]/ K	$T_{S_X-S_C}$/ K	T_{S_C-N}/ K	T_{N-I}/ K	$\Delta H_{S_X-S_C}$/ J g^{-1}	ΔH_{S_C-N}/ J g^{-1}	ΔH_{N-I}/ J g^{-1}
2a	*c*	301	360	370	3.0	5.5	2.2
2b	*c*	297	356	366	2.8	5.0	2.0
2c	*c*	298	356	367	2.5	4.5	1.8
2d	316	302	352	361	2.3	1.7	1.3

[a] Transition temperatures and entropies (T, ΔH). Phases: S_X, smectic F or I; S_C, smectic C; N, nematic; I, isotropic. [b] Melting of the poly(2-isobutyl vinyl ether) block. [c] Not detected.

Table 5. Phase Transition Temperatures[a] of Copolymers 3

sample	T_m[b]/K	$T_{S_X-S_C}$/K	T_{S_C-N}/K	T_{N-I}/K
3a	300	306	333	343
3b	293	301	*c*	*c*

[a] Phases: S_X: smectic F or I; S_C, smectic C; N, nematic; I, isotropic phases. [b] Melting of the poly((*S*)-2-methylbutyl vinyl ether) block. [c] Not determined because of the overlapping peaks from 311 to 344 K.

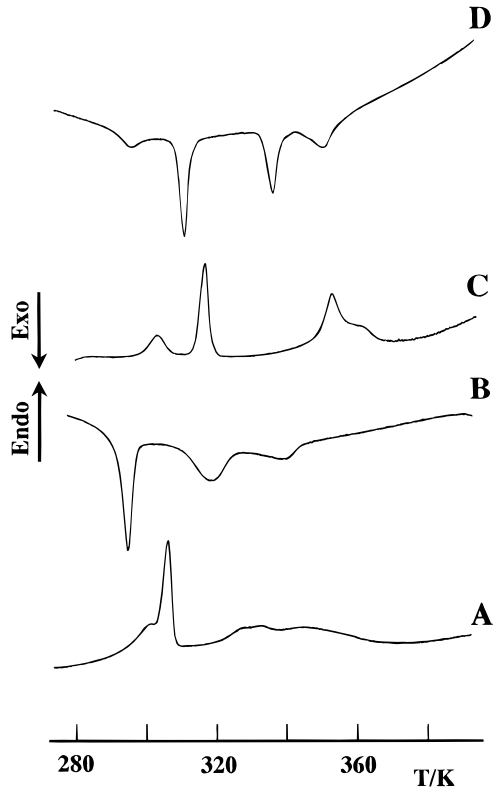

Figure 11. DSC second heating and first cooling curves (10 K min^{-1}) of copolymers **2d** (C, D) and **3b** (A, B).

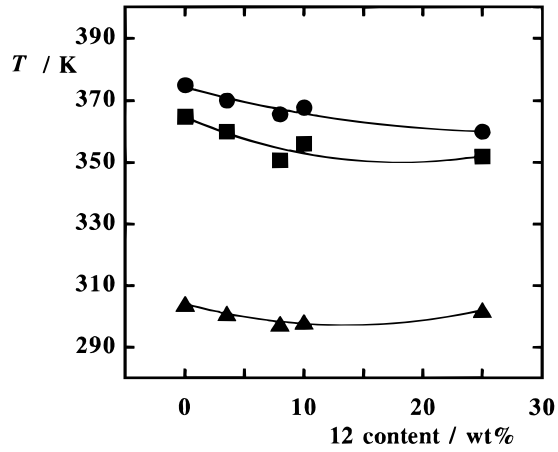

Figure 12. Trends of the smectic X−smectic C (▲), smectic C−nematic (■), and nematic−isotropic (●) transition temperatures as a function of the isobutyl vinyl ether (**12**) content in block copolymers **2**.

11C). On cooling, all these transitions are reversible. A similar behavior is shown by block copolymer **3b** except for the fact that the crystallization exotherm of the poly((*S*)-2-methylbutyl vinyl ether) block is superimposed on the S_C-S_X transition of the LC poly(vinyl ether) block (Figure 11B). Figures 12 and 13 illustrate the trends of the S_X-S_C, S_C-N, and N−I transition temperatures and enthalpies (ΔH), respectively, for block copolymers **2** as a function of the isobutyl vinyl ether (**12**) unit content. The LC phase transition temperatures decrease regularly with increasing poly(isobutyl vinyl ether) block content. In a parallel fashion, the enthalpy changes associated with the LC transitions are lower than the ones expected on the basis of the weight composition of the block copolymers. The observation of distinct transitions associated with both different blocks suggests that they are microphase

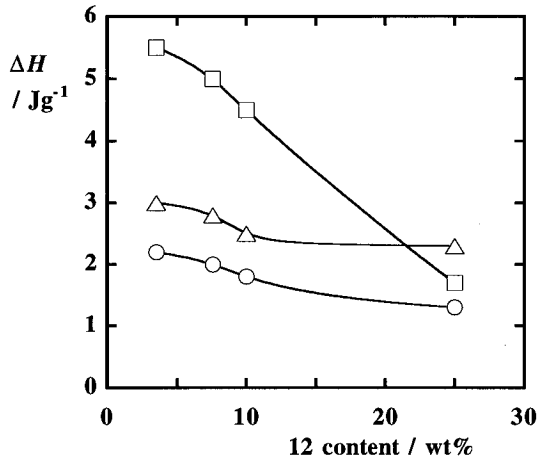

Figure 13. Trends of the smectic X−smectic C (△), smectic C−nematic (□), and nematic−isotropic (○) transition enthalpies as a function of the isobutyl vinyl ether (**12**) content in block copolymers **2**.

separated within the solid and the LC phases. However, the dependence of the transition temperatures and entropies on the copolymer composition coupled with the observation that the width of the DSC curves of block copolymers **2** and **3** is substantially wider than the one of polymers **1** strongly suggests the existence of interactions or miscibility between the different blocks.

Concluding Remarks

A series of LC poly(vinyl ether)s **1** with different molar masses and two series of block copoly(vinyl ether)s were synthesized by living cationic polymerization using HI/I_2 as the initiating system. By properly adjusting the ratio between the monomer and initiator concentrations, it was possible to produce polymers with predetermined molar mass values and copolymers with tailored block lengths and compositions. All the polymer **1** samples form smectic F (or I), smectic C, and nematic mesophases. The phase transition parameters of polymer **1** samples increase sligthly with increasing number average molar mass up to a saturation value of $M_n = 6000$ g mol^{-1}. This result further confirms the general trend observed for side-chain LC polymers with narrow molar mass distribution. The basic mesophase sequence observed in polymers **1** is also recognized for AB diblock copolymers **2** and **3** comprising a non-LC block and an LC block analogous to polymers **1**. This clearly indicates that the chemically different blocks are segregated within the solid and LC phases.

Acknowledgment. This work was done with financial support from the European Community, *Human Capital and Mobility* Network Program.

References and Notes

(1) *Side Chain Liquid Crystal Polymers*; McArdle, C. B., Ed.; Blackie: Glasgow, 1989.
(2) (a) Kreuder, W.; Webster, W. O.; Ringsdorf, H. *Makromol. Chem., Rapid Commun.* **1986**, *7*, 5. (b) Hefft, M.; Springer, J. *Makromol. Chem., Rapid Commun.* **1990**, *11*, 397.
(3) (a) Bohnert, R.; Lutz, P.; Finkelmann H. *Makromol. Chem., Rapid Commun.* **1993**, *14*, 139. (b) Bohnert, R.; Finkelmann H. *Macromol. Chem. Phys.* **1994**, *195*, 689.
(4) (a) Sagane, T.; Lenz, R. W. *Polym. J. (Jpn).* **1988**, *20*, 923. (b) Sagane, T.; Lenz, R. W. *Macromolecules* **1989**, *22*, 3763.
(5) Percec, V.; Tomazos D. *Adv. Mater.* **1992**, *4*, 548.
(6) (a) Chiellini, E.; Galli, G.; Cioni, F. *Ferroelectrics* **1991**, *114*, 223. (b) Chiellini, E.; Dossi, E.; Galli, G.; Solaro, R.; Gallot, B. *Macromol. Chem. Phys.* **1995**, *196*, 3859.

(7) Kostromin, S. G.; Cuong, N. D.; Garina, E. S.; Shibaev, V. P. *Mol. Cryst. Liq. Cryst.* **1990**, *193*, 177.
(8) (a) Rodriguez-Parada, J. M.; Percec, V. *J. Polym. Sci. Polym. Chem. Ed.* **1986**, *24*, 1363. (b) Percec, V.; Tomazos, D. *Polym. Bull. (Berlin)* **1991**, *25*, 47. (c) Rodenhouse, R.; Percec, V. *Polym. Bull. (Berlin)* **1991**, *25*, 47. (d) Percec, V.; Gomes, A. S.; Lee, M. *J. Polym. Sci., Part A: Polym. Chem.* **1991**, *29*, 1615. (e) Percec, V.; Lee, M.; Tomazos, D. *Polym. Bull. (Berlin)* **1992**, *28*, 9. (f) Percec, V.; Zheng, Q. *Polym. Bull. (Berlin)* **1994**, *32*, 249.
(9) (a) Jonsson, H.; Andersson, H.; Sundell, P. E.; Gedde, U. W.; Hult, A. *Polym. Bull. (Berlin)* **1993**, *32*, 249. (b) Jonsson, H.; Sundell, P. E.; Percec, V.; Gedde, U. W.; Hult, A. *Polym. Bull. (Berlin)* **1991**, *25*, 649.
(10) Percec, V.; Lee, M. *J. Macromol. Sci., Pure Appl. Chem.* **1992**, *A29*, 723.
(11) (a) Adams, J.; Gronski, W. *Makromol. Chem., Rapid Commun.* **1989**, *10*, 553. (b) Adams, J.; Sänger, J.; Tefehne, C.; Gronski, W. *Makromol. Chem., Rapid Commun.* **1994**, *15*, 879.
(12) Komiya, Z.; Schrock, R. R. *Macromolecules* **1993**, *26*, 1387.
(13) Radzilowski, L. H.; Wu, J. L.; Stupp, S. I. *Macromolecules* **1993**, *26*, 879.
(14) (a) Zaschke, B.; Frank, W.; Fischer, H.; Schmutzler, K.; Arnold, M. *Polym. Bull. (Berlin)* **1991**, *27*, 1. (b) Arnold, M.; Poser, S.; Fisher, H.; Frank, W.; Utschick, H. *Makromol. Chem., Rapid Commun.* **1994**, *15*, 487.
(15) (a) Galli, G.; Chiellini, E.; Yagci, Y.; Serhatli, E. I.; Laus, M.; Angeloni, A. S.; Bignozzi M. C. *Makromol. Chem., Rapid Commun.* **1993**, *14*, 185. (b) Angeloni, A. S.; Bignozzi, M. C.; Laus, M.; Chiellini, E.; Galli, G. *Polym. Bull. (Berlin)* **1993**, *31*, 387. (c) Galli, G.; Chiellini, E.; Laus, M.; Bignozzi, M. C.; Angeloni, A. S.; Francescangeli, O. *Macromol. Chem. Phys.* **1994**, *195*, 2247.
(16) Galli, G.; Chiellini, E.; Angeloni, A. S.; Laus, M. *Trends Polym. Sci.* **1994**, *2*, 244.
(17) Lorenzi, G. P.; Benedetti, E.; Chiellini, E. *Chim. Ind. (Milan)* **1964**, *46*, 1474.
(18) Braun, D.; Herr, R. P.; Arnold, N. *Makromol. Chem., Rapid Commun.* **1987**, *8*, 359.
(19) (a) Miyamoto, M.; Sawamoto, M.; Higashimura, T. *Macromolecules* **1984**, *17*, 265. (b) Higashimura, T.; Miyamoto, M.; Sawamoto, M. *Macromolecules* **1985**, *18*, 611.
(20) Kennedy, J. P. *Macromol. Chem., Macromol Symp.* **1991**, *47*, 55.
(21) (a) Benattar, J. J.; Moussa, F.; Lambert, M. *J. Chim. Phys., Chim. Biol.* **1983**, *80*, 99. (b) Gane, P. A. C.; Leadbetter, A. J.; Benattar, J. J.; Moussa, F.; Lambert, M. *Phys. Rev. A* **1981**, *24*, 2694.
(22) Tabrizian, M.; Bunel, C.; Vairon, J.-P.; Friedrich, C.; Noel, C. *Makromol. Chem.* **1993**, *194*, 891.
(23) Stevens, H.; Rehage, G.; Finkelmann, H. *Macromolecules* **1984**, *14*, 1543.
(24) Percec, V.; Tomazos, D.; Pugh, C. *Macromolecules* **1989** *22*, 3259.

MA951641V